View metadata, citation and similar papers at core.ac.uk
brought to you by CORE
provided by Queen Mary Research Online

Broadband Matching of Nuclear Quadrupole Resonance Detector Using Non-Foster Circuits

Wanlin Li, Khalid Z. Rajab
School of Electronic Engineering and Computer Science,
Queen Mary University of London,
London, United Kingdom.
k.rajab@qmul.ac.uk

Kaspar Alhoefer
Faculty of Science and Engineering,
Queen Mary University of London,
London, United Kingdom.

Blaz Zupancic, Jamie Barras
Department of Informatics
Kings College London,
London, United Kingdom.

***Abstract*— A new class of nuclear quadrupole resonance (NQR) detector based on non-Foster circuits (NFCs) is introduced. NQR is a solid-state radio frequency spectroscopic technique, allowing the detection of different substances based on their spectral profiles. Recently, non-Foster circuits have received significant interest for broadband impedance matching of small antennas; this principle will be used to develop highly matched, broadband antennas, which will allow very quick NQR detection from 1 MHz to 6 MHz.**

Keywords*— Nuclear Quadrupole Resonance, Non-Foster Circuits, Negaitive Impedance Converter, Stability

I. INTRODUCTION

Antennas are fundamentally limited by the balance between their bandwidth and size; wide bandwidth requires a relatively large antenna and this could be a serious problem for some portable devices [1,2]. The negative impedance converter (NIC) is an important class of Non-Foster Circuits (NFCs) [3,4] in which the input impedance is negative, allowing for negative resistors, inductors or capacitors. This is extremely beneficial for cancelling out the inductance or capacitance of small antennas, which limits their performance. Thus NICs can be applied to cancel reactive components of an electrically small antenna (ESA), enabling broadband matching impedance matching [5].

In this paper we present a novel application of NIC impedance matching for nuclear quadrupole resonance (NQR) sensing applications. NQR refers to the energy level transition of the nucleus when excited with an external electromagnetic field (or excitation signal) [6]. The nucleus then emits a signal of a specific frequency, normally from 0-6 MHz. Since different nuclei or even identical nuclei in the structures of different substances could have a different NQR frequency, this characteristic spectrum could be an effective method to identify different substances. However, the NQR signal is normally quite weak and is significantly degraded by background noise. In order to overcome this noise multiple measurements are taken to improve SNR to useable levels. High-Q matching circuits are used to detect the spectral profile, however this leads to long LC ringing times which, coupled with the large number of measurements results in impractically long measurements times. To overcome this, we propose the use of NICs to achieve broadband matching of the detector and obtain maximum power for weak signal detection. This has two benefits: it will increase the bandwidth over which resonances can be detected; and the low-Q circuit will significantly decrease ringing time, and shorten detection time within the NQR receiving system [7].

II. DESIGN AND SIMULATION RESULT OF NIC

A typical NQR detecting device [8] is shown in Figure 1 (as the receiver). In this case, the NQR signal induced through mutual inductance can be calculated. The reactance X_m can be determined to match to the preamplifier characteristic impedance R_0 (50 Ω). Through selection of passive LC components, a highly resonant condition will be met, however through use of negative impedance components broadband matching may be achieved.

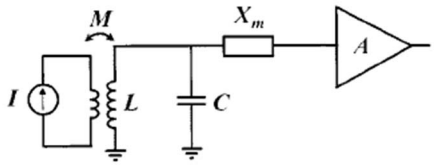

Fig. 1. The equivalent circuit of a typical NQR detecting device, The sample is regarded as a current loop and is mutually coupled to the probe coil by the mutual inductance M, NIC is applied in the reactance part X_m. *(figure caption)*

While there are a number of different NIC topologies – including recently proposed designs based on resonant tunneling diodes [9] and Graphene FETs [10] – at VHF there are two that are relatively common and suitable for this application: operational amplifier (op-amp); and dual bipolar junction transistors (BJTs).

A. Op-amp-based NIC

The op-amp NIC is a one-port operational amplifier circuit with a load impedance, called negative impedance converter with current inversion (INIC), as shown in Figure 2. INIC is a

non-inverting amplifier, which is a particular mode of the differential amplifier. The inverting input is grounded and the non-inverting input is equalized with V_S. Two resistors (R_1, R_2) are placed as the voltage dividers and one resistor (R_3) is set between the output and its input. The input impedance can be regarded as

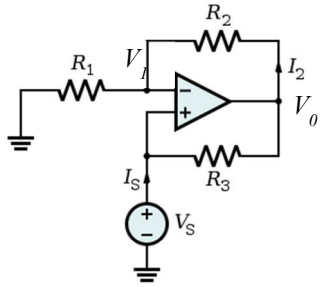

Fig. 2. Negative impedance converter circuit based on op-amp model. *(figure caption)*

The input impedance of the circuit in Figure 2 can be regarded as $-R_3*R_1/R_2$, which gives a negative resistance. The resistors in the circuit can also be replaced by capacitors to obtain the negative capacitance model and negative inductance model.

The Advanced Design System (ADS) simulation results of the negative resistance, negative capacitance and negative inductance are shown in Figure 3(a)-(c) respectively. As for Figure 3(a) that with a load of 500 Ω and the biasing voltage of 18 V, the circuit displays a negative resistance between 1 MHz to 10 MHz. Figure 3(b) displays a negative capacitance with the load of 100 *pF* and the same biasing voltage. Figure 3(c) displays a negative inductance with the load of 15 *μH* and the same biasing voltage within the operating frequency. Figure 3(d) shows the voltage comparison between the source and the load using MSO-X 2002A Mixed Signal Oscilloscope.

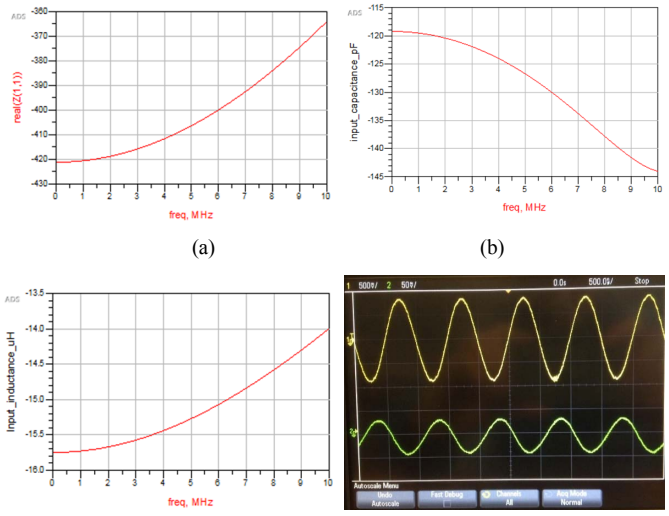

Fig. 3. (a) ADS simulation result of negative resistance op-amp model with 500 Ω load. (b) ADS simulation result of negative capacitance op-amp model with 100 *pF* load. (c) ADS simulation result of negative inductance op-amp model with 15 *μH load*. (d) Voltage display of source(yellow plot) and load(green plot) using the oscilloscope. *(figure caption)*

B. *BJT Mode*

The Linvill NIC [11] was presented in 1953 and has been covered extensively elsewhere [4,5].

The Advanced Design System (ADS) simulation results of the negative resistance, negative capacitance and negative inductance are shown in Figure 4(a) (b) (c) respectively. As for Figure 4(a) that with a load of 200 Ω and the biasing voltage of 14 V, the circuit displays a negative resistance between 1 MHz to 50 MHz. Figure 3(b) displays a negative capacitance with the load of 20 *pF* and the same biasing voltage. Figure 3(c) displays a negative inductance with the load of 5 *μH* and the same biasing voltage within the operating frequency. Figure 3(d) shows the voltage comparison between the source and the load using MSO-X 2002A Mixed Signal Oscilloscope.

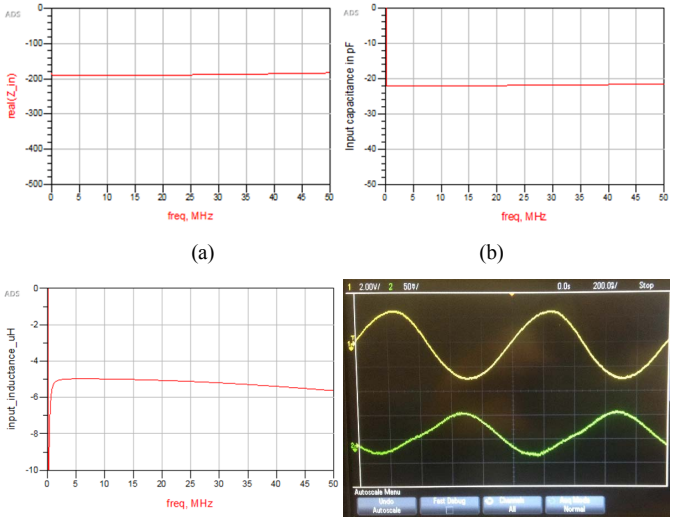

Fig. 4. (a) ADS simulation result of negative resistance BJT model with 200 Ω load. (b) ADS simulation result of negative capacitance BJT model with 20 *pF* load. (c) ADS simulation result of negative inductance BJT model with 5 *μH load*. (d) Voltage display of source(yellow plot) and load(green plot) using the oscilloscope. *(figure caption)*

III. NIC Stability Discussion

Stability is an important factor in NIC design, as they can very easily go unstable under certain circumstances. A stability analysis [4,12] based on the location of the poles on the complex s-plane is applied in the analysis of NICs, with a positive real part predicting instability within the NIC. In order to determine the location of the poles of the typical NICs, for example in the Linvill transistor model, the transfer function of the NIC is found as $H(s)=Y(s)/X(s)$, where $Y(s)$ is the Laplace transform of the response of the circuit and $X(s)$ is the Laplace transform of the input. The location of the zeros and poles of the transfer function in the complex s-plane will predict the stability of the circuits according to the Nyquist criterion. When the real part of the poles of the transfer function are negative, which means they are all in the left half of the complex s-plane, then the response in time domain will lead to a decaying exponential. Otherwise if the poles are in the right half of the complex plane, the time

domain response will have a growing exponential (oscillation with increasing amplitude) which indicates the instability. If the real part of the poles is zero, then this will result in an oscillation with constant amplitude.

If we consider the parasitic effects in a practical model, the procedure can become very complex and it will be difficult to directly find the corresponding roots from the high order polynomials. The Nyquist contour can be used efficiently to determine the stability of a system [12]. The transfer function is expressed as the product of the source impedance $Z_s(s)$ and load admittance $Y_l(s)$, and when plotted in the complex plane, will encircle the -1 point N times, where $N=Z-P$, where Z and P are the number of zeros and poles respectively. Here, counterclockwise encirclements are considered to be positive and clockwise encirclements are considered to be negative. The number of clockwise encirclements of -1 represents the number of unstable poles of the system. Thus there will be no encirclements of -1 for a stable system. All the impedance poles of an open-circuit stable NIC will be placed in the left half of the plane and is represented by the source impedance, all the admittance poles of a short-circuit stable NIC will be placed in the left half of the plane and is represented by the load admittance. Further details are given in [12].

IV. Design And Simulation Result of NQR Device

NQR detector has been widely used for a range of applications including the detection of expired pharmaceuticals and explosives ordinance detection. However, the practical application is limited by the amount of time it takes to make a measurement. Low measurement frequency and high environmental noise levels require high Q circuits [14], which implies a large number of relatively slow measurements. It would therefore be extremely beneficial to significantly decrease the measurement time and obtain a broadband matching with the use of the non-Foster characteristic of NIC.

A. Common Method of NQR Detection

An excellent explosives detector would be able to give an instant scanning for a given area and then report the result correctly. In response to the characteristics of NQR, a particular detecting system was introduced using a probe coil to provide electromagnetic shielding to reduce or even eliminate radio frequency interference (RFI). An antenna probe is composed of a tuning circuit with high Q factor and impedance matching circuit. A general functional block diagram is shown in Figure 5. As can be seen that NQR detecting system consists of main control computer (MCC), signal generator, high-power transmitter, probe coil, pre-amplifier, analogue receiver and digital receiver.

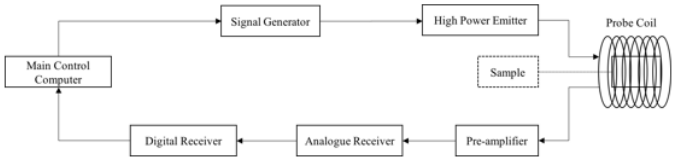

Fig. 5. The components of NQR system. *(figure caption)*

B. Design and Simulation Result of NQR Device

The NQR signals are always very weak and they are captured by their influence on an RF probe coil. Both the random thermal noise caused by the coil and in the first stage of the preamplifier could restrict the SNR of the receiving NQR signal and the low SNR therefore hampers the commercial use of NQR detection. The equivalent circuit of the probe coil and sample is shown in Figure 1, the parameters within the figure are L=13 μH, C=1 pF, the resistance of the coil R=185 $m\Omega$, M=325 nH. The comparison between using passive matching method and NIC method to replace X_m is shown below.

1) Use passive matching method

The load impedance can be calculated as $Z_L=R_L+X_L$=0.184+j81.68 Ω, since the impedance of the pre-amplifier can be regarded as Z_0=50 Ω, we use the type of matching circuit shown in Figure 6.

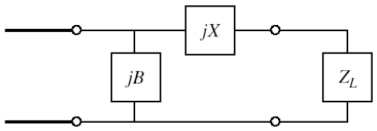

Fig. 6. Matching with Lumped elements. *(figure caption)*

The corresponding parameters are calculated as B=±0.329 Ω^{-1} and X=-78.65 Ω. So there are two types of matching circuits, the first one uses a series capacitor of 2.02 nF and a shunt capacitor of 52.34 nF. The second one uses a series capacitor of 1.9 nF and a shunt inductor of 0.32 μH. The ADS simulation results of the two types of circuits are similar, Figure 7 shows the passive matching circuits using two capacitors and the result of AC case and transient case respectively.

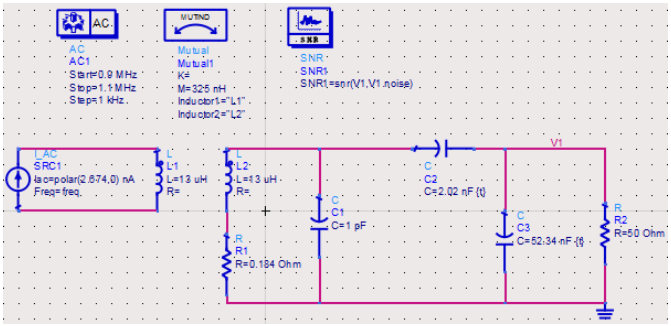

(a)

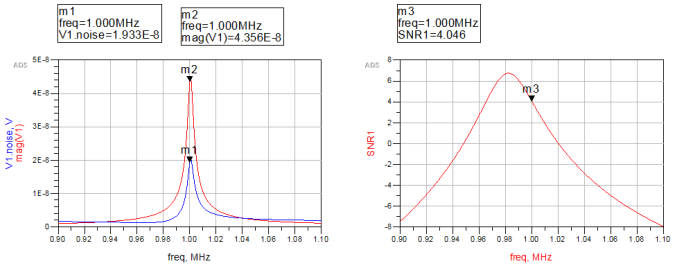

(b)

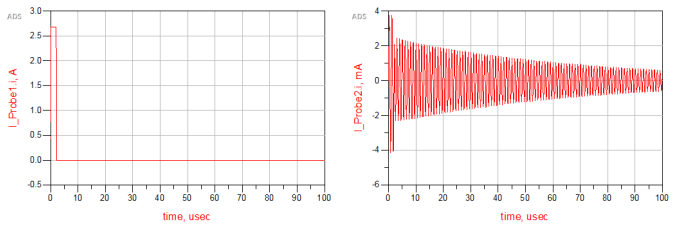

(c)

Fig. 7. (a) ADS schematics of Lumped matcing circuit using two capacitors. (b) ADS AC simulation result of Lumped matcing circuit using two capacitors. (c) ADS transient simulation result of Lumped matcing circuit using two capacitors. *(figure caption)*

The AC simulation result (see Figure 7(b)) shows that the circuit has a narrow match at 1 MHz at which the slope is negative. The signal to noise ratio (SNR) is around 4 dB and the voltage at the output terminal is on the order of around 43 nV. The transient result (see Figure 7(c)) shows that it takes a while for the signal to dampen due to the high Q, which means that the repeated measurements will take a long time.

2) Use NIC matching method

NIC circuits can be used to replace the Lumped element as the non-Foster matching topology is shown in Figure 8 in which NIC is a one-port network and the load of NIC (NFCs) is the exact value of the reactance of the load impedance Z_A.

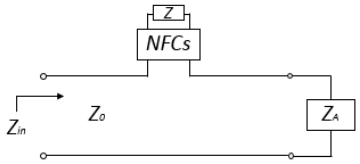

Fig. 8. Non-Foster matching topology. *(figure caption)*

Therefore each Lumped element in the original matching circuit (Figure 7(a)) can be replaced with another new NIC component which can be regarded as a negative reactance value. So there will also be two cases because of the two scenarios of the passive matching. The first case uses a series inductor of -13.48 μH and a shunt capacitor of -53.6 nF. The second case uses a series inductor of -15.2 μH and a shunt inductor of -0.25 μH. The ADS simulation results of the two types of circuits are similar, Figure 9 shows the NIC matching circuits using one inductor and one capacitor and the result of AC case and transient case respectively.

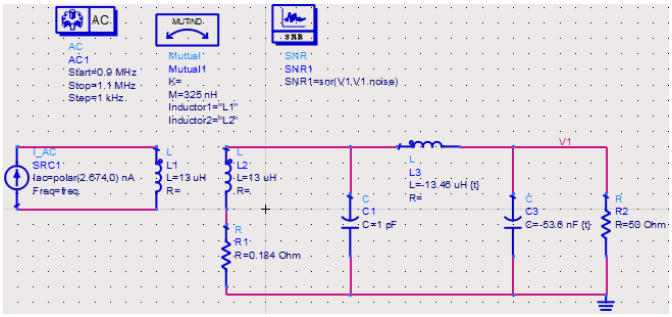

(a)

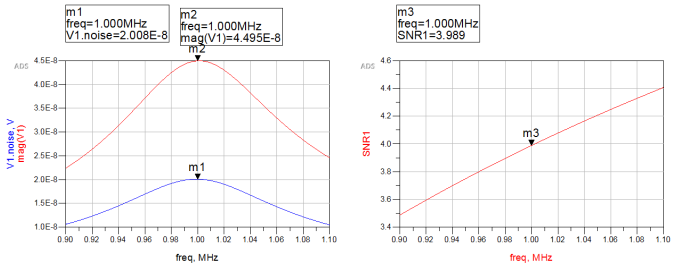

(b)

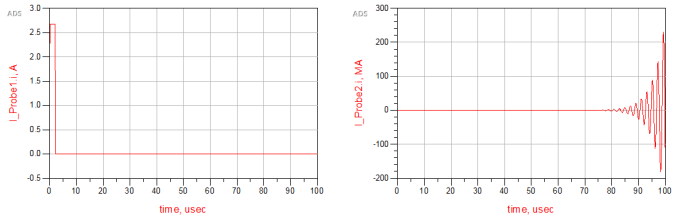

(c)

Fig. 9. (a) ADS schematics of NIC matcing circuit using one inductor and one capacitor. (b) ADS AC simulation result of NIC matcing circuit using one inductor and one capacitor. (c) ADS transient simulation result of NIC matcing circuit using one inductor and one capacitor. *(figure caption)*

The AC simulation result (see Figure 9(b)) shows some differences that NICs provide a wider matching compared with the passive matching method (see Figure 8(b)), this means the voltage is maximised across the whole band, rather than just 1 MHz. Noise characterization is important, and particularly so with active elements such as the NIC [13,14]. The SNR is about 4 dB which is similar to the use of lumped-section matching and the voltage at the output terminal is on the same order with Lumped matching (45 nV). The transient result (see Figure 10(c)) shows if we use NIC to replace all the passive Lumped elements, the transient result can be unstable, this may due to the overcompensation of any of the elements. The overcompensation can be relieved by selecting the proper value of each components.

V. CONCLUSIONS

The simulation results from Agilent ADS present apparent NIC behavior for both operational amplifier NIC and bipolar junction transistor NIC within the VHF-low range as all of the six modes give a gratifying negative value of the corresponding load. Based on the NICs results and the parameters of the NQR detector coil, the use of NICs can be applied into the NQR receiving part for broadband matching. The use of NICs has the benefits of significantly enhancing the band over which maximum power transfer is possible due to the impedance matching. This allows for uncertainty at an exact resonant frequency and also ensure the measurement of multiple resonances. The use of NICs could also reduce the time for signal to decay due to a relatively low Q within the system. This ensures the multiple measurements to be performed far more quickly. However, noise and stability issues of NICs must be accounted for within simulation, and these can be crucial when designing the actual microwave networks.

ACKNOWLEDGMENTS

The authors thank Mr. Deepak Singh Nagarkoti and Mr. Peter Lawrence Alizadeh for their assistance in the design and manufacture of the NICs.

REFERENCES

[1] H. A. Wheeler, "Fundamental Limitations of Small Antennas," Proceedings of the IRE, vol. 35, no. 12, pp. 1479-1484, 1947.

[2] L. J. Chu, "Physical limitations of omnidirectional antennas," Journal of Applied Physics, vol. 19, pp. 1163-1175, 1948.

[3] O. O. Tade, P. Gardner, and P. S. Hall, 'Negative impedance converters for broadband antenna matching', in Microwave Conference (EuMC), 2012 42nd European, 2012, pp. 613–616.

[4] K. Z. Rajab, Y. Hao, D. Bao, C. G. Parini, J. Vazquez, and M. Philippakis, "Stability of active magnetoinductive metamaterials," Journal of Applied Physics 108 (5), 054904, 2010.

[5] S. Sussman-Fort and R. Rudish, "Non-Foster Impedance Matching of Electrically-Small Antennas," IEEE Trans. Antennas and Propagat., vol. 57, no. 8, pp. 2230-2241, Aug. 2009.

[6] J. A. S. Smith, "Nuclear quadrupole resonance spectroscopy, general principles," J. Chem. Educ., vol. 48, pp. 39-49, 1971.

[7] J. B. Miller, B. H. Suits, A. N. Garroway, and M. A. Hepp, "Interplay among recovery time, signal, and noise: Series- and parallel-tuned circuits are not always the same", Concepts Magn. Reson., vol. 12, pp. 125–136, 2000.

[8] A. N. Garroway, "Remote sensing by nuclear quadrupole resonance," IEEE Transactions on Geoscience and Remote Sensing, vol. 39, no. 6, pp. 1108-1118, 2001.

[9] D. Nagarkoti, Y. Hao, D. P. Steenson, L. Li, E. H. Linfield, and K. Z. Rajab, "Design of broadband non-Foster circuits based on resonant tunneling diodes," IEEE Antennas and Wirless Propagat. Lett., vol. 15, pp. 1398-1401, 2016.

[10] J. Tian, D. S. Nagarkoti, K. Z. Rajab and Y. Hao, "Graphene-based tunable non-Foster circuit for VHF applications," AIP Advances 6 (6), 065202, 2016.

[11] J. G. Linvill, "Transistor Negative-Impedance Converters," Proceedings of the IRE, vol. 41, no. 6, pp. 725-729, 1953.

[12] K. Z. Rajab, Y. F. Fan, and Y. Hao, "Characterization of active metamaterials based on negative impedance converters," Journal of Optics, vol. 14, no. 11, 114004, Nov. 2012, 8 pages.

[13] Y. F. Fan, K. Z. Rajab, and Y. Hao, "Noise analysis of broadband active metamaterials with non-Foster loads," Journal of Applied Physics, vol. 113, 233905, 2013.

[14] Y. Fan, D. S. Nagarkoti, K Z. Rajab, Y. Hao, H. C. Zhag, T. J. Cui, "Wave propagation in reconfigurable broadband gain metamaterials at microwave frequencies," Journal of Applied Physics 119 (19), 194904, 2016.